ISSN 1029-9599, Physical Mesomechanics, 2018, Vol. 21, No. 1, pp. 6–14. © Pleiades Publishing, Ltd., 2018.
Original Text © J. Nowak, M. Kaczmarek, 2017, published in Fizicheskaya Mezomekhanika, 2017, Vol. 20, No. 5, pp. 10–17.

Modelling Deep Tonometry of Lymphedematous Tissue

J. Nowak and M. Kaczmarek*

Institute of Mechanics and Applied Computer Science, Kazimierz Wielki University, Bydgoszcz, 85-074 Poland
** e-mail: mkk@ukw.edu.pl*

Received March 29, 2017

Abstract—Indentation testing, also refereed to as tonometry in medical diagnostics, is one of the most frequently used methods for studying the properties of soft biological tissues. In the case of lymphedematous tissues, characterized by abnormal accumulation of excess interstitial fluid, the indentation method constitutes an objective alternative for the standard manual palpation test, that is used for evaluation of elastic modulus and time dependent tissue response related to finding parameters of effective compression therapy. This paper focuses on the numerical modelling of a deep indentation test for which the flat cylindrical tip with a surface area of 1 cm^2 penetrates the tissue at a constant rate until 1 cm depth is reached. The indentation generates large deformations of skin and subcutaneous tissue and squeezing of part of the interstitial fluid from the compressed region. The skin is modelled as an isotropic neo-Hookean solid and subcutaneous tissue is modelled as a fluid saturated porous matrix. The effective stress law, isotropic neo-Hookean elastic matrix and the Darcy's type of interaction force between phases are adopted for the subcutaneous tissue. The finite element simulations deliver results for time dependent indentation force and pore pressure under the indenter for different and relevant to real tissues properties. The role of the properties and the presence of skin are analysed. The values of maximum reaction force and relaxation time are compared and evaluated as descriptors of mechanical properties of tissues.

DOI: 10.1134/S1029959918010022

Keywords: indentation test, large deformations, porous materials, soft lymphedematous tissue, finite element analysis, diagnostic method

1. INTRODUCTION

Lymphedema is a disease, which is a consequence of the obstruction of lymph transport in or into lymphatic system caused by such factors as inflammation, excision of lymph nodes or irradiation. This type of edema is related to accumulation of capillary filtrate with proteins and other components which constitute substrates for growing subcutaneous tissue with excess of stagnant fluid [1]. Among the conservative therapeutic modalities, which are effective to minimize the edema of limbs there are different types of external compression, particularly intermittent pneumatic compression (IPC) [2–4]. In most cases the technique uses a number of chambers, which are sequentially inflated starting from the most distal one. As a result the fluid in compressed tissue is translated to proximal regions. In order to assure the effective intermittent pneumatic compression action proper pressures and times of compression must be applied. The therapeutic parameters are dependent on properties of tissue such as elastic modulus and permeability and cannot exceed physiologically acceptable limits [1]. One of the methods that are most frequently used for evaluation of mechanical properties of soft tissues is the indentation test [5–17], which is used also for lymphedematous tissue [5–11]. The method is a more advanced and objective version of the manual palpation test. The indentation method, in medical diagnostics called also tonometry, can be a load or displacement control test. When both the maximum values of force or displacement and creep or relaxation periods are observed the technique can be useful for evaluation of elastic modulus and hydraulic properties of tissue.

In the literature there are available numerous analytical models for classical or rebound indentation, developed for small deformation cases [e.g. 12–14],

and numerical models of indentation test for large deformation range, see e.g. [15–17]. Then, however, in most cases a single-phase material model of tissues is considered.

Taking into account the fact that the deep indentation test generates not only large deformations of tissues but also squeezing of the interstitial fluid from the compressed region of subcutaneous tissue the finite strain model of the fluid saturated solid matrix is used. Following the model proposed by Li et al. [18] the effective stress law along with the isotropic neo-Hookean elastic matrix and the Darcy's type of interaction force between phases are adopted for the subcutaneous tissue. The skin is modelled as an isotropic neo-Hookean solid. The indentation of the flat cylindrical tip with a surface area of 1 cm^2, which penetrates the tissue at constant rate until 1 cm depth is reached, is simulated.

The finite element technique implemented within COMSOL Multiphysics environment delivers results for time dependent indentation force and pore pressure under the indenter for different and relevant to real tissues properties. The role of tissue properties and the presence of skin are analysed. The maximum reaction force, as well as the relaxation times is determined. The results are discussed in light of fits obtained for linear model of indentation into finite solid layer [12] and poroelastic homogeneous material [19].

2. DEEP TONOMETRY OF SOFT TISSUES

The considered deep indentation method applied for lymphedematous tissues [2] uses a flat cylindrical tip with a surface area of 1 cm^2, which is pressed against tissues at constant rate of approximately 1 mm per second to the depth of 1 cm. In the simplest case the maximum force is recorded by a dynamometer [2] (Fig. 1a). In more advanced solutions the microprocessor-controlled device (Fig. 1b) allows for displacement control according to ramp-hold type function (Fig. 1c) and acquisition of time dependence of the force on indenter [16]. Then, the peak force and the relaxation time can be determined and used as the descriptors of mechanical state of the tissue.

The measurements are usually performed for selected localizations of the internal side of limbs. The examples of results for deep tonometry performed before and after application of intermittent pneumatic compression for a patient with diagnosed lymph edema are shown in Fig. 2.

As it can be noticed from Fig. 2 the indentation test shows that for lymphedematous tissues the compression therapy lowers elastic modulus of tissue, the peak force and influences the properties, which determine relaxation time.

3. MATHEMATICAL MODEL

To model indentation test it is assumed that the deformation takes place for a layer of skin and subcutaneous tissue, while muscles and bones remains undeformable. The skin is modelled as homogeneous isotropic neo-Hookean solid. For the subcutaneous tissue the two-phase model of porous matrix filled with fluid is adopted. The elastic matrix (mostly cells and fibers) is homogeneous and isotropic neo-Hookean material and viscous fluid (interstitial fluid) has properties of water. Gravity and inertial forces are disregarded. The finite strain poroelastic model developed by Li et al. [18] is used with matrix deformation and pore fluid pressure as dependent variables.

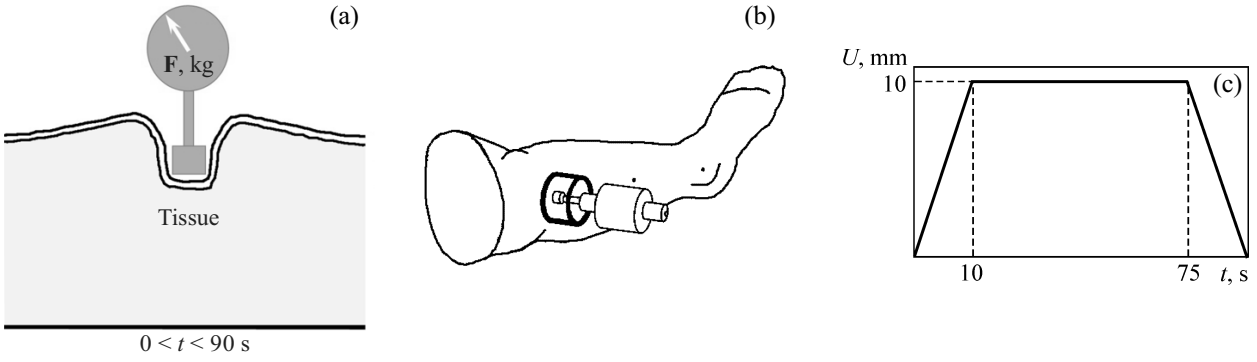

Fig. 1. Schematics of simple tonometry test with dynamometer (a) and microprocessor-controlled device (b) along with ramp-hold type displacement function of indenter (c).

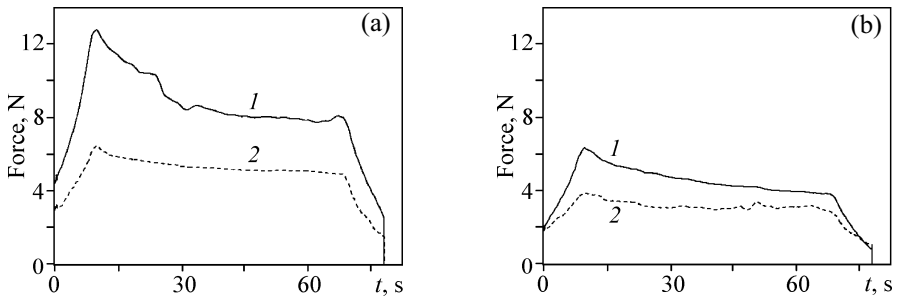

Fig. 2. Examples of results from deep tonometry tests for a patient with lymphedema of lower limb recorded at ankle (a) and in the middle of calf (b) before (*1*) and after intermittent pneumatic compression (*2*).

The equilibrium equation formulated in reference configuration takes on the form:

$$\mathrm{DIV}\,\mathbf{P}^i = \mathbf{0}, \tag{1}$$

where index *i* refers to skin (s) or subcutaneous tissue (t), the operator DIV is defined in the reference configuration, $\mathbf{P}^i$ denotes the first Piola–Kirchhoff stress tensor. In the case of subcutaneous tissue the tensor $\mathbf{P}^i$ is the total stress, which includes stresses in matrix and fluid and can be represented by effective stress principle

$$\mathbf{P}^{\mathrm{t}} = \tilde{\mathbf{P}}^{\mathrm{t}} - B\theta(\mathbf{F}^{\mathrm{t}})^{-T}, \tag{2}$$

where $\tilde{\mathbf{P}}^{\mathrm{t}}$ is the effective stress tensor, θ stands for the Kirchhoff pressure in fluid, related to Cauchy pore fluid pressure *p*

$$\theta = J^{\mathrm{t}} p, \tag{3}$$

where *B* is the effective stress coefficient, $J^{\mathrm{t}} = \det \mathbf{F}^{\mathrm{t}}$ and $\mathbf{F}^{\mathrm{t}}$ is the deformation gradient of solid matrix.

For homogeneous isotropic neo-Hokean materials the stress tensors are related to elastic strain energy functions W^i

$$\mathbf{P}^{\mathrm{s}} = 2\mathbf{F}^{\mathrm{s}} \cdot \frac{\partial W^{\mathrm{s}}}{\partial \mathbf{C}^{\mathrm{s}}}, \quad \tilde{\mathbf{P}}^{\mathrm{t}} = 2\mathbf{F}^{\mathrm{t}} \cdot \frac{\partial W^{\mathrm{t}}}{\partial \mathbf{C}^{\mathrm{t}}}, \tag{4}$$

where

$$W^i = \frac{\mu^i}{2}[\mathrm{tr}\,\mathbf{C}^i - 3] - \mu^i \ln J^i + \frac{\lambda^i}{2}\ln^2 J^i, \tag{5}$$

$\mathbf{C}^i$ are the right Cauchy–Green deformation tensors, $J^{\mathrm{t}} = \det \mathbf{F}^{\mathrm{t}}$ are the determinants of the deformation gradient, μ^i and λ^i are elastic material constants. Taking into account equation (2) for the case of subcutaneous tissue the elasticity constants correspond to drained deformation of the matrix.

The model of flow of interstitial fluid in tissue is formulated in current configuration combining the mass balances for the tissue (for both components), linear momentum for pore fluid and a set of constitutive equations [18]. The mass balance for the tissue reads

$$\frac{1-\varphi}{\rho_{\mathrm{m}}}\frac{\mathrm{d}\rho_{\mathrm{m}}}{\mathrm{d}t} + \frac{\varphi}{\rho_{\mathrm{f}}}\frac{\mathrm{d}\rho_{\mathrm{f}}}{\mathrm{d}t} + \mathrm{div}\,\mathbf{v}_{\mathrm{m}} + \frac{1}{\rho_{\mathrm{f}}}\mathrm{div}(\varphi\rho_{\mathrm{f}}\mathbf{u}) = 0, \tag{6}$$

where $\varphi, \rho_{\mathrm{m}}, \rho_{\mathrm{f}}$ are porosity, true densities of solid matrix and pore fluid, $\mathbf{v}_{\mathrm{m}}$ and $\mathbf{u}$ are velocities of solid matrix and pore fluid with respect to the matrix. The convective component of the total time derivative $\mathrm{d}/\mathrm{d}t$ includes the matrix velocity and the operator div is defined in current configuration.

The linear momentum of pore fluid (with neglected inertial and gravity forces and operator grad defined in current configuration) is

$$-\varphi\,\mathrm{grad}\,p + \mathbf{h} = \mathbf{0}, \tag{7}$$

where $\mathbf{h}$ is the vector of viscous interaction force between matrix and fluid. The constitutive equations expressing the barotropic fluid, the dependence of density of matrix on its dilatation, and relating the interaction force between phases to relative velocity are

$$\frac{\mathrm{d}\rho_{\mathrm{f}}}{\rho_{\mathrm{f}}} = \frac{\mathrm{d}p}{K_{\mathrm{f}}}, \tag{8}$$

$$\frac{1-\varphi}{\rho_{\mathrm{m}}}\frac{\mathrm{d}\rho_{\mathrm{m}}}{\mathrm{d}t} = -\frac{K}{K_{\mathrm{m}}}\mathrm{div}\,\mathbf{v}_{\mathrm{m}}, \tag{9}$$

$$\mathbf{h} = -\varphi^2\eta\mathbf{k}^{-1}\mathbf{u}, \tag{10}$$

where parameters K_{f}, K_{m} and K denote bulk modulus of fluid, material of matrix and porous matrix, η is fluid dynamic viscosity, and $\mathbf{k}$ is the permeability tensor, which for the isotropic case is reduced to a scalar permeability.

Then, using Eqs. (6)–(10) and formulas allowing for transition from current to reference configuration (the operator GRAD appears then instead of grad) the differential equation for pore fluid pressure coupled with volumetric deformation of matrix in reference configuration is

$$B\frac{\mathrm{d}J}{\mathrm{d}t}+\frac{J\varphi}{K_\mathrm{f}}\frac{\mathrm{d}}{\mathrm{d}t}\left(\frac{\theta}{J}\right)-\frac{1}{\eta}\mathrm{DIV}\left[\bar{\mathbf{k}}\mathrm{GRAD}\left(\frac{\theta}{J}\right)\right]=0, \quad (11)$$

where the effective stress coefficient $B=1-K/K_\mathrm{m}$ and the spatial changes of fluid density ρ_f were neglected. The coupled system of Eqs. (1)–(5) and (11) describes deformation of solid matrix and pore fluid pressure of soft tissue.

4. NUMERICAL SIMULATIONS AND ANALYSIS

The numerical simulations were performed for a cylindrical geometry of the considered system (Fig. 3a). The system is composed of a layer of skin with thickness h = 1 mm and layer of subcutaneous tissue having thickness H = 30 mm. The diameter of the cylinder amounts to d = 120 mm. The surface of the cylindrical flat indenter as in real tests is 1 cm^2. The simulations by finite element method are performed within the COMSOL Multiphysics environment.

4.1. Initial and Boundary Conditions

It is assumed that initially there is no prestrain in skin and tissue matrix, and the pore fluid pressure is equal to zero. The following set of boundary conditions is formulated using axial symmetry of the system and notation shown in Fig. 3b:

a) the outflow of pore fluid is possible only in radial r direction along the circumferential boundary DF,

b) the bottom of the indenter AB and particles of skin underneath are displaced into tissue only in axial z direction,

c) particles at the bottom of the sample EF can displace frictionless only in radial direction,

d) the load on the tissue is applied throughout the indenter, which is displaced with constant velocity 1 mm/s until it reaches depth U_max = 10 mm,

e) for the interface between the skin and subcutaneous tissue CD the displacements and stresses are continuous.

In order to compare the values of pore fluid pressure for different material parameters the control point J located on symmetry axis 0.5 mm under the skin is introduced.

4.2. Material Parameters

The numerical studies were performed assuming a set of parameters representing a wide range of elastic modulus of skin and matrix of subcutaneous tissue, as well as permeability of the latter material. The data were adopted from the papers devoted to soft tissues using linear elasticity or poroelasticity models [4, 16]. The material constants μ^i and λ^i for skin and subcutaneous tissue (in linear elasticity called Lame coefficients) were determined assuming the well-known relations with Young modulus E_s and E_t and Poisson's ratio ν_s and ν_t, of the material components and have better physical meaning. For skin the Young modulus amounts to 0.25, 0.50 or 1.00 MPa, while the Poisson's ratio is constantly equal to 0.49. For subcutaneous tissue the drained Young modulus is 25, 75 or 150 kPa while the drained Poisson's ratio amounts 0.33. The value of permeability coefficient k is assumed as 5×10^{-14}, 15×10^{-14} and 45×10^{-14} m^2. Taking into account that bulk elastic modulus of matrix is much larger than for porous matrix B = 1. Porosity of subcutaneous tissue is φ = 0.05, while densities of matrix and pore fluid as well as viscosity of pore fluid are assumed as for water.

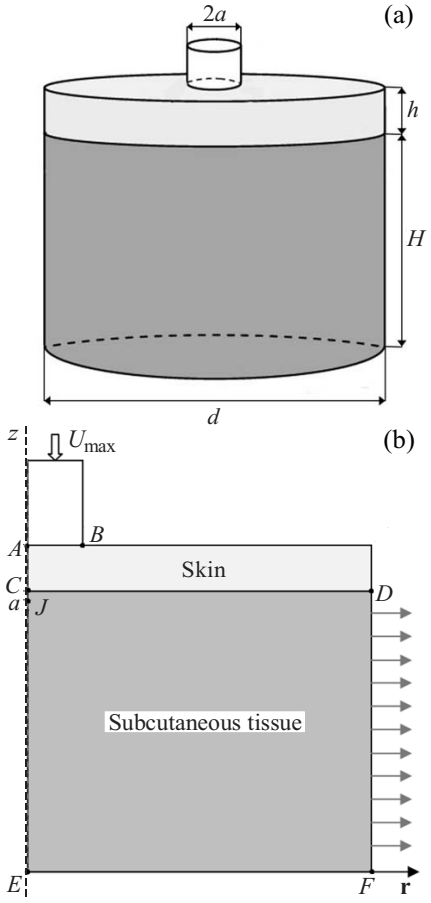

Fig. 3. Geometry of the simulated system (a) and half of its vertical cross-section (b).

4.3. Results for Model with Skin

The simulations are focused on time dependence of the reaction force on indenter exerted by tissue during tonometry tests. Moreover, for better understanding of the interrelations between the properties of the matrix and the pore fluid the pressure at control point J will be also analysed.

The first series of results (Figs. 4 and 5) concerns simulations performed for different elastic modulus of subcutaneous tissue ($E_t = 25$, 75 and 150 kPa), or its permeability ($k = 5\times10^{-14}$, 15×10^{-14}, and 45×10^{-14} m^2) keeping constant elastic modulus of skin (E_s = 0.25 MPa).

The results shown in Fig. 4 are in qualitative agreement with examples of experimental data presented in Fig. 2. Initially in the period of penetration of indenter into tissue the reaction force increases fast and then it follows the relaxation period associated with slow decrease of force. The level of reaction force is significantly influenced by elastic modulus, however because of nonlinearity it is not proportional to Young modulus of tissue. The detailed analysis of the relaxation periods indicates that the initial slope of the curves, which usually determines the relaxation time do not decrease strictly monotonically with elastic modulus of matrix. This kind of behaviour could be expected from linear poroelasticity [19] when the load period is very short. The permeability of subcutaneous tissue has limited influence on the reaction force (Fig. 4b) although it is visible that the lower permeability the higher maximum force. The comparison of results for relaxation period also proves a lack of monotonic increase of the relaxation time with decreasing permeability (see Sect. 4.5), which seems to be again related to relatively long load period.

Figure 5 illustrates the role of elastic modulus and permeability of subcutaneous tissue for pressure changes in pore fluid at the control point localized on the symmetry axis 0.5 mm under the skin. The dependence of pressure on time both in the load period and relaxation period is strongly nonlinear. The increasing elastic modulus of tissue causes an increase of the pressure, first of all in the load period, and then the observed changes are not very significant. The permeability of tissue is a much more important factor that influences the complete time dependence of pressure. The results show that distributions of stress between matrix and fluid are not fixed and they change for different loads, particularly for relaxation periods.

Both from the reaction force and pressure dependence on time it results that the load period, which amounts to 10s, is too long to assume that the load period is

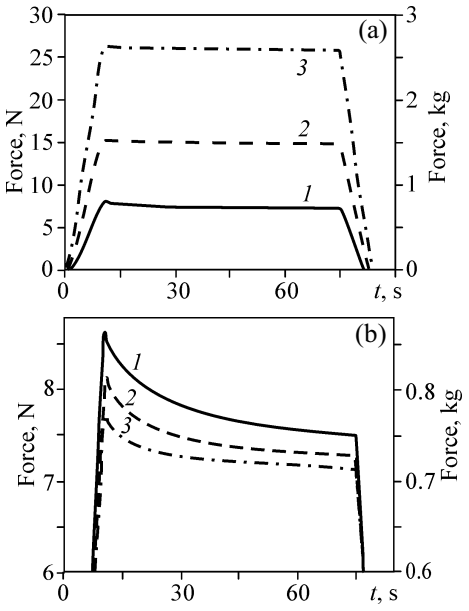

Fig. 4. Reaction force on indenter as the function of time for different elastic modulus E_t = 25 (*1*), 75 (*2*), and 150 kPa (*3*) of subcutaneous tissue (a) and permeability $k = 5\times10^{-14}$ (*1*), 15×10^{-14} (*2*) and 45×10^{-14} m^2 (*3*) (b) while elastic modulus of skin remains constant.

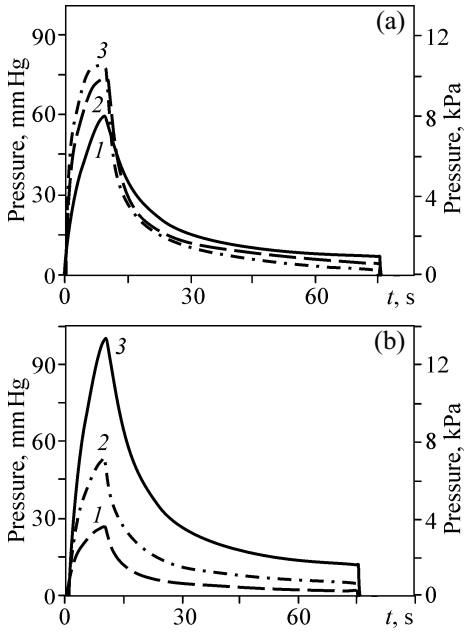

Fig. 5. Pore fluid pressure at control point J as the function of time for different elastic modulus E_t = 25 (*1*), 75 (*2*), 150 kPa (*3*) of subcutaneous tissue (a) and permeability $k = 5\times10^{-14}$ (*1*), 15×10^{-14} (*2*), 45×10^{-14} m^2 (*3*) (b) while elastic modulus of skin remains constant (E_s = 0.25 MPa).

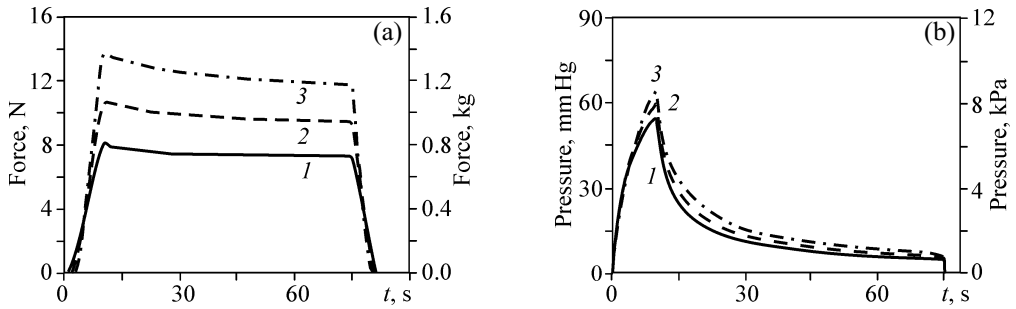

Fig. 6. Reaction force on indenter (a) and pore fluid pressure (b) as the functions of time for different elastic modulus of skin $E_s = 0.25$ (*1*), 0.50 (*2*), 1.00 MPa (*3*) and constant elastic modulus and permeability of subcutaneous tissue ($E_t = 25$ kPa, $k = 15\times10^{-14}$ m^2).

purely undrained deformation. On the other hand, one should notice relatively large values of the maximum pressure in pore fluid (the maximum physiologically accepted pressures should not exceed 120 mm Hg) and this is the factor, which does not allow shortening the load period.

The role of elasticity of skin is studied changing its Young modulus ($E_s = 0.25, 0.50$ and 1.00 MPa), while Poisson ratio is always constant, $\nu_s = 0.49$. The elastic modulus and permeability of subcutaneous tissue are also assumed to be constant ($E_t = 25$, 75 and 150 kPa, $k = 5\times10^{-14}$, 15×10^{-14} and 45×10^{-14} m^2). Figure 6 presents dependence of the reaction force on indenter and pore fluid pressure in control point on time for the above conditions.

The increase of the elastic modulus of skin (Fig. 6a) results in a change of the maximum reaction force on indenter from 8.12 to 10.80 and then 13.73 N. There is also an increase of relaxation time observed. The variation of pore fluid pressure at control point due to increase of elastic modulus of skin is not significant and is mostly monitored as change of the maximum pressure and variation in relaxation period.

4.4. Results for Model without Skin

For further evaluation of the role of skin in deep tonometry the model neglecting skin is considered. The assumptions for the field equations, initial and boundary conditions corresponding to subcutaneous tissue are not changed. From the computational point of view the model without skin has appeared much less stable than the model, which includes skin, and adjustment of relative tolerance of the finite element solver was necessary. This generated some disturbances visible in solutions close to the maximum values of force or pressure.

Figure 7 presents changes in reaction force on indenter as the functions of time for different elastic modulus and permeability of tissue. One can notice that contrary to the model with skin now the maximum force is roughly proportional to Young modulus. The differences in relaxation time for tissues with different permeability are more significant (see also Sect. 4.5) and like for the model with skin the permeability influences the maximum value of reaction force.

The dependence of pore fluid pressure on time in control point for different elasticity and permeability

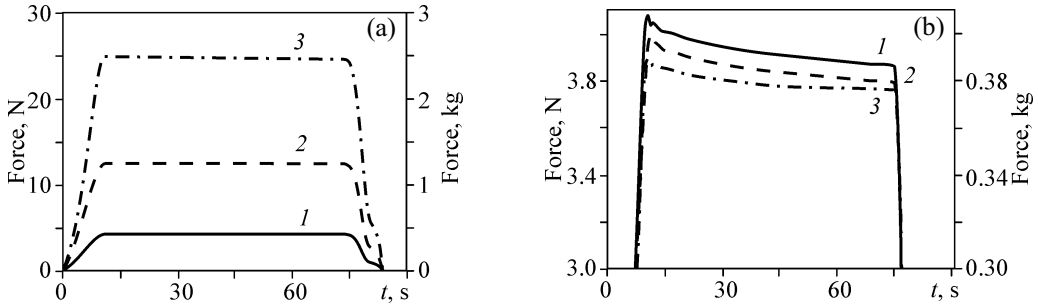

Fig. 7. Reaction force on indenter as the function of time for different elastic modulus $E_t = 25$ (*1*), 75 (*2*), 150 kPa (*3*) of subcutaneous tissue (a) and permeability $k = 5\times10^{-14}$ (*1*), 15×10^{-14} (*2*), 45×10^{-14} m^2 (*3*) (b). The presence of skin is neglected in this model.

of tissue is presented in Fig. 8. The maximum pressures are lower than for the model with skin and are not proportional to elasticity of tissue (like it is for the reaction force).

The results for different permeability (Fig. 8b) indicate that the pore pressure in the model without skin (maximum values are between 20 and 100 mm Hg) is lower than for the model with skin (maximum values are between 30 and 130 mm Hg). The time when pressure reaches constant values is approximately inversely proportional to permeability.

4.5. Analysis of Maximum Reaction Force and Relaxation Time

In the linear model of indentation into saturated poroelastic materials with a short load period to assure the condition of undrained deformation two descriptors of mechanical properties of tissue are usually considered: the maximum reaction force and the relaxation time [19]. The descriptors are tightly related to elasticity and permeability of studied porous materials. The results of the performed finite strain simulations of deep tonometry could be used to evaluate the usefulness of the descriptors in the large deformation case.

The comparison of the maximum reaction force for the modelled system with and without skin assuming

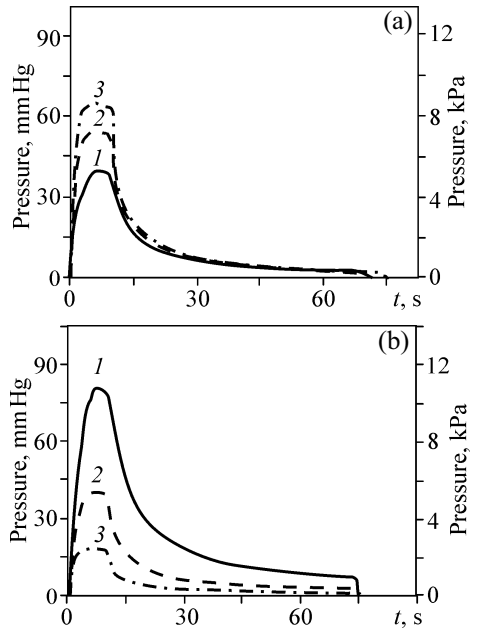

Fig. 8. Pore fluid pressure at control point J as the function of time for different elastic modulus $E_t = 25$ (*1*), 75 (*2*), 150 kPa (*3*) of subcutaneous tissue (a) and permeability $k = 5\times10^{-14}$ (*1*), 15×10^{-14} (*2*), 45×10^{-14} m^2 (*3*) (b). The presence of skin is neglected in this model.

three values of Young modulus of subcutaneous tissue is presented in Table 1. Additionally, the table contains results obtained from approximated formula received from the linear model of indentation of the flat cylindrical tip into a homogeneous incompressible elastic layer with boundary conditions corresponding to the considered indentation problem [12]:

$$F_{\max} = 8\mu a U_{\max}\left[0.98472 + 0.91345\frac{a}{H} + 0.29577\left(\frac{a}{H}\right)^2 - 0.11993\left(\frac{a}{H}\right)^3 + \frac{2.3904}{1000}\left(\frac{a}{H}\right)^4 - \frac{8.1689}{10000}\left(\frac{a}{H}\right)^5\right], \quad (12)$$

where μ is the shear stiffness of tissue, H denotes thickness of the layer, a is the radius of indenter, and $U_{\max}$ stands for the indentation depth. Although the elastic parameters of the matrix (E_t, ν_t) given in Table 1 refer to drained conditions it should be noticed that for the applied, relatively short load period the maximum reaction force approximates the force for undrained conditions. This justifies also the comparison of the solution for two phase model with the model assuming incompressible solid. It is seen from Table 1 that the maximum reaction forces for models with and without skin (see also Figs. 4a and 7a) become closer for higher stiffness of tissue and this corresponds to decreasing role of skin. Although the maximum reaction force determined from the finite strain model with skin is not strictly proportional to Young modulus its values may represent changing stiffness of tissue. The predictions of the linear model overestimates the reaction force determined for the model without skin but differences are not larger than 15%.

Taking into account the relaxation period of the indentation test into homogeneous poroelastic layer the finite element simulations performed within the linear model and short load step [19] allowed to find the

Table 1. Comparison of the maximum reaction forces for load period of tonometry from the finite strain models (subcutaneous tissue $\nu_t = 0.33$, $k = 15\times10^{-14}$ m^2) and the linear model

Young modulus of subcutaneous tissue E_t, kPa	Maximum reaction force $F_{\max}$, N		
	Finite strain model without skin	Finite strain model with skin ($h = 1$ mm, $E_s = 0.25$ MPa, $\nu_s = 0.49$)	Linear model, Eq. (12)
25	4.22	8.12	4.80
75	12.71	15.47	14.41
150	25.23	26.51	28.82

Table 2. Comparison of the characteristic relaxation times for relaxation period of tonometry from the finite strain models (subcutaneous tissue $E_t = 25$ kPa, $\nu_t = 0.33$) and the linear model

Permeability of subcutaneous tissue k, m^2	Characteristic relaxation times τ, s		
	Finite strain model without skin	Finite strain model with skin ($h = 1$ mm, $E_s = 0.25$ MPa, $\nu_s = 0.49$)	Linear model, Eq. (14)
5×10^{-14}	264.0	39	19.5
15×10^{-14}	60.3	27	4.5
45×10^{-14}	40.5	26	2.2

following fit of the reaction force

$$F_r = F_0 - M\,\mathrm{erf}\left[\sqrt{t_r/\tau} - 0.23 t_r/\tau + 0.02(t_r/\tau)^{3/2}\right], \quad (13)$$

where F_0 is the initial (maximum) value of the force, M is a constant representing difference between F_0 and the reaction force for infinite time, erf stands for the error function, t_r is the time variable measuring duration of the relaxation period, and τ is the characteristic relaxation time. The relaxation time was then calculated as

$$\tau = \frac{a^2(1-2\nu)\eta}{2\mu k(1-\nu)}. \quad (14)$$

The results of simulations obtained for the relaxation part of the reaction force for deep tonometry with different values of permeability (data shown in Figs. 4b and 7b) and Eq. (13) were used in order to find with help of numerical optimization implemented in Matlab environment the unknown parameters F_0, m and τ. The values of the characteristic relaxation time for models with skin and without skin are compared in Table 2. Additionally the values obtained directly from Eq. (14) are given.

Table 2 shows large discrepancies between relaxation times determined from the finite strain models of tissue with and without skin and even larger differences when compared to predictions of Eq. (14). Qualitatively similar results are obtained when we use as the fitting exponential or bi-exponential functions. Thus, contrary to the linear model with short ramp step the relaxation time cannot be considered as a simple indicator of permeability of subcutaneous tissue determined from deep tonometry.

5. CONCLUSIONS

The finite strain simulations of deep tonometry tests into a layer of lymphedematous tissue were considered assuming a poroelastic model of the subcutaneous layer. The simulations are done for models with and without skin and the range of parameters expected for real cases. It was shown that the reaction force depends mostly on elastic properties of subcutaneous tissue. The role of skin is significant for low stiffness of tissue and becomes less important for stiff subcutaneous tissues. The permeability of subcutaneous tissue influences the time dependence of the reaction force in relaxation period of the tonometry test but also the maximum reaction force. The latter effect is the result of relatively long load period and fact that the undrained condition for ramp loaded fluid saturated tissue matrix is not satisfied in the period. The same reason causes that the standard descriptors of stiffness and permeability of tissues for indentation within the small strain range: the maximum reaction force and the relaxation time have limited value as the indicators of properties of tissues when they are determined from deep tonometry. In particular the relaxation time is no longer simply related to permeability.

Assuming that the deep tonometry is the preferred type of indentation method for lymphedematous tissues (the loading conditions on tissues during the test are similar as for the basic therapeutic modality which constitutes the intermittent pneumatic compression) it seems to be necessary to make efforts for finding parameters, which correspond to hydromechanical properties of tissues. It concerns particularly the indicator of permeability, which in the present studies is assumed constant but should be also considered as the property that changes with deformation of tissue. In spite of the classical indentation techniques the rebound indentation tests should be taken into account (see e.g. [13, 20]), which results do not depend on thickness of the studied layer and the indenter shape. Further works are also necessary in order to find in the tonometry tests such diagnostic parameters, which minimize or quantify the contribution of skin.

ACKNOWLEDGMENTS

This work was partially supported by the National Science Centre (grant UMO-2013/11/B/ST8/03589) and the National Centre for Research and Development (grant PBS3/B9/46/2015).

REFERENCES

1. Olszewski, W.L., Jain, P., Ambujam, G., Zaleska, M., Cakała, M., and Gradalski, T., Tissue Fluid Pressure and

Flow During Pneumatic Compression in Lymphedema of Lower Limbs, *Lymph. Res. Biology*, 2011, vol. 9, pp. 77–83.
2. Zaleska, M., Olszewski, W.L., and Durlik, M., The Effectiveness of Intermittent Pneumatic Compression in Long-term Therapy of Lymphedema of Lower Limbs, *Lymph. Res. Biology*, 2014, vol. 12, pp. 103–109.
3. Zaleska, M., Olszewski, W.L., Cakała, M., Ćwikła, J., and Budlewski, T., Intermittent Pneumatic Compression Enhances Formation of Edema Tissue Fluid Channels in Lymphedema of Lower Limbs, *Lymph. Res. Biology*, 2015, vol. 13, pp. 146–153.
4. Kaczmarek, M., Olszewski, W.L., Nowak, J., and Zaleska, M. The Hydromechanics of Edema Fluid in Lymphedematous Lower Limb during Intermittent Pneumatic Compression, *Lymph. Res. Biology*, 2015, vol. 13, pp. 260–267.
5. Chen, H.C., O'Brien, B., Pribaz, J.J., and Roberts, A.H.N., The Use of Tonometry in the Assessment of Upper Extremity Lymphoedema, *Brit. J. Plast. Surgery*, 1988, vol. 41, pp. 399–402.
6. Kar, S.K., Kar, P.K., and Mania, J., Tissue Tonometry: a Useful Tool for Assessing Filarial Lymphedema, *Lymphology*, 1992, vol. 25, pp. 55–61.
7. Liu, N. and Olszewski, W.L., Use of Tonometry to Assess Lower Extremity Lymphedema, *Lymphology*, 1992, vol. 25, pp. 155–158.
8. Zheng, Y.P., Mak, A.F.T., and Lue, B., Objective Assessment of Limb Tissue Elasticity: Development of a Manual Indentation Procedure, *J. Rehabilitation Res. Develop.*, 1999, vol. 36, pp. 71–85.
9. Mayrowitz, H.N., Assessing Lymphedema by Tissue Indentation Force and Local Tissue Water, *Lymphology*, 2009, vol. 42, pp. 88–98.
10. Suchiro, K., Morikage, N., Murakami, M., Yamashita, O., Samura, M., and Hamano, K., Significance of Ultrasound Examination of Skin and Subcutaneous Tissue in Secondary Lower Extremity Lymphedema, *Ann. Vascular Diseases*, 2013, vol. 6, pp. 180–188.
11. Bates, D.O., Levick, J.R., and Mortimer, P.S., Quantification of Rate and Depth of Pitting in Human Edema Using an Electronic Tonometer, *Lymphology*, 1994, vol. 27, pp. 159–172.
12. Yang, F., Indentation of an Incompressible Elastic Film, *Mech. Mater.*, 1998, vol. 30, pp. 275–286.
13. Argatov, I. and Mishuris, G., An Analytical Solution for a Linear Viscoelastic Layer Loaded with a Cylindrical Punch: Evaluation of the Rebound Indentation Test with Application for Assessing Viability of Articular Cartilage, *Mech. Res. Comm.*, 2011, vol. 38, pp. 565–568.
14. Argatov, I., An Analytical Solution of the Rebound Indentation Problem for an Isotropic Linear Viscoelastic Layer Loaded with a Spherical Punch, *Acta Mech.*, 2012, vol. 223, pp. 1441–1453.
15. Liu, Y., Kerdok, A.E., and Howe, R.D., A Nonlinear Finite Element Model of Soft Tissue Indentation, *Proc. Medical Simulation: International Symposium-ISMS. Lect. Notes Comput. Sci.*, 2004, vol. 3078, pp. 67–76.
16. Iivarinen, J.T., Korhonen, R.K., Julkunen, P., and Jurvelin, J.S., Experimental and Computational Analysis of Soft Tissue Elastic Modulus in Forearm Using a Manual Indentation Device, *Med. Eng. Phys.*, 2011, vol. 33, pp. 1245–1253.
17. Zhang, M., Zheng, Y.P., and Mak, A.F.T., Estimating of the Effective Young's Modulus of Soft Tissues from Indentation Test—Nonlinear Finite Element Analysis of Effects of Friction and Large Deformation, *Med. Eng. Phys.*, 1997, vol. 19, pp. 512–517.
18. Li, Ch., Borja, R.I., and Regueiro, R.A., Dynamics of Porous Media at Finite Strain, *Comput. Meth. Appl. Mech. Eng.*, 2004, vol. 193, pp. 3837–3870.
19. Lin, Y.Y. and Hu, B.W., Load Relaxation of a Flat Rigid Circular Indenter on a Gel Half Space, *J. Non-Cryst. Solids*, 2006, vol. 352, pp. 4034–4040.
20. Argatov, I. and Popov, V.L., Rebound Indentation Problem for a Viscoelastic Half-Space and Axisymmetric Indenter—Solution by the Method of Dimensionality Reduction, *Z. Angew. Math. Mech.*, 2016, vol. 96, no. 8, pp. 956–967.